

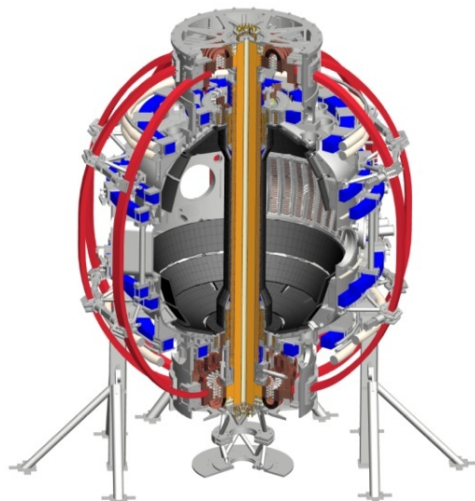
# Rotation and kinetic resonance effects on the spherical tokamak ideal-wall limit\*

**Jon Menard (PPPL)**

Z. Wang, Y. Liu (CCFE), S. Kaye, J.-K. Park,  
J. Berkery (CU), S. Sabbagh (CU)  
and the NSTX Research Team

**55<sup>th</sup> Annual Meeting of the APS-DPP**  
**November 11, 2013**  
**Denver, Colorado**

\*This work supported by US DoE contract DE-AC02-09CH11466

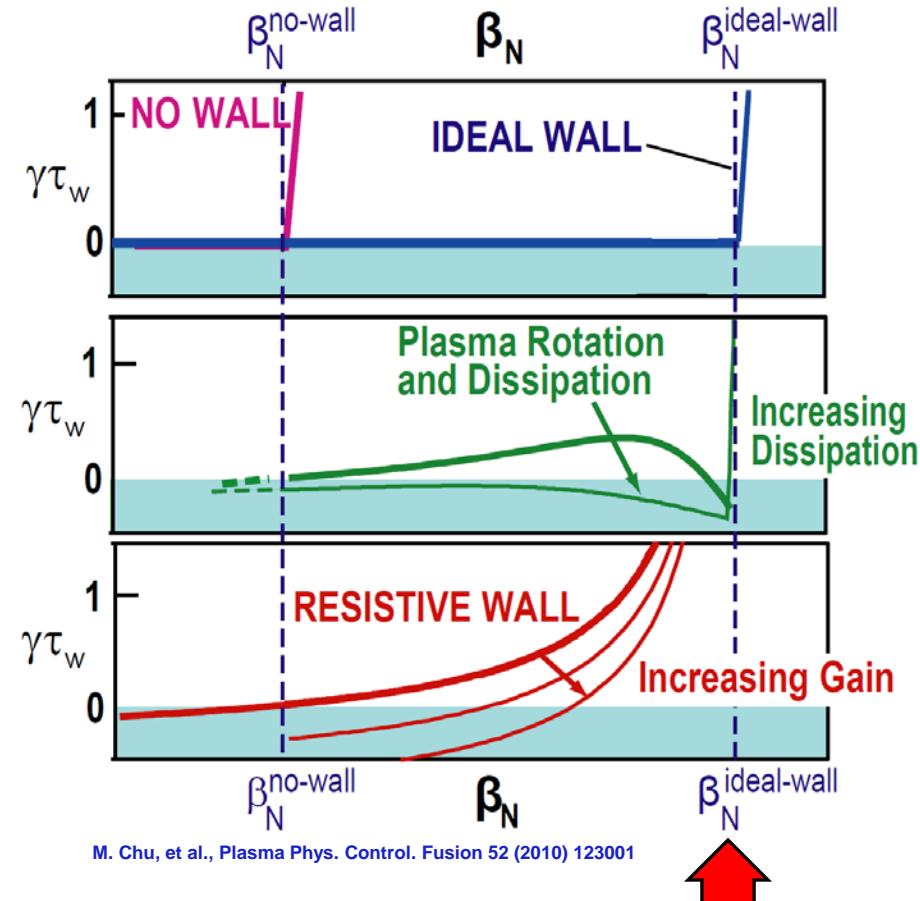


Coll of Wm & Mary  
Columbia U  
CompX  
General Atomics  
FIU  
INL  
Johns Hopkins U  
LANL  
LLNL  
Lodestar  
MIT  
Lehigh U  
Nova Photonics  
Old Dominion  
ORNL  
PPPL  
Princeton U  
Purdue U  
SNL  
Think Tank, Inc.  
UC Davis  
UC Irvine  
UCLA  
UCSD  
U Colorado  
U Illinois  
U Maryland  
U Rochester  
U Tennessee  
U Tulsa  
U Washington  
U Wisconsin  
X Science LLC

Culham Sci Ctr  
York U  
Chubu U  
Fukui U  
Hiroshima U  
Hyogo U  
Kyoto U  
Kyushu U  
Kyushu Tokai U  
NIFS  
Niigata U  
U Tokyo  
JAEA  
Inst for Nucl Res, Kiev  
Ioffe Inst  
TRINITI  
Chonbuk Natl U  
NFRI  
KAIST  
POSTECH  
Seoul Natl U  
ASIPP  
CIEMAT  
FOM Inst DIFFER  
ENEA, Frascati  
CEA, Cadarache  
IPP, Jülich  
IPP, Garching  
ASCR, Czech Rep

# Pressure-driven kink limit is strong physics constraint on maximum fusion performance

$$P_{\text{fusion}} \propto n^2 \langle \sigma v \rangle \propto p^2 \propto \beta_T^2 B_T^4 \propto \beta_N^4 B_T^4 (1 + \kappa^2)^2 / A f_{\text{BS}}^2$$



- Modes grow rapidly above kink limit:
  - $\gamma \sim 1\text{-}10\%$  of  $\tau_A^{-1}$  where  $\tau_A \sim 1\mu\text{s}$
- Superconducting “ideal wall” can increase stable  $\beta_N$  up to factor of 2
- Real wall resistive  $\rightarrow$  slow-growing “resistive wall mode” (RWM)
  - $\gamma \tau_{\text{wall}} \sim 1 \rightarrow$
  - ms instead of  $\mu\text{s}$  time-scales
- RWM can be stabilized with:
  - kinetic effects (rotation, dissipation)
  - active feedback control

**This talk: study ideal-wall mode (IWM) in plasmas w/ stable RWM**

# Background

- Characteristic growth rates and frequencies of RWM and IWM
  - RWM:  $\gamma\tau_{\text{wall}} \sim 1$  and  $\omega\tau_{\text{wall}} < 1$
  - IWM:  $\gamma\tau_A \sim 1\text{-}10\%$  ( $\gamma\tau_{\text{wall}} \gg 1$ ) and  $\omega\tau_A \sim \Omega_\phi\tau_A$  (1-30%) ( $\omega\tau_{\text{wall}} \gg 1$ )
- Kinetic effects important for RWM (J. Berkery invited TI2.02, Thu AM)
  - Publications: Berkery, et al. PRL 104 (2010) 035003, Sabbagh, et al., NF 50 (2010) 025020
- Rotation and kinetic effects largely unexplored for IWM
  - Such effects generally higher-order than fluid terms ( $\nabla p$ ,  $J_\parallel$ ,  $|\delta B|^2$ , wall)
- **Calculations for NSTX indicate both rotation and kinetic effects can modify IWM stability limits**
  - High toroidal rotation generated by co-injected NBI in NSTX
    - Fast core rotation:  $\Omega_\phi / \omega_{\text{sound}}$  up to  $\sim 1$ ,  $\Omega_\phi / \omega_{\text{Alfven}}$   $\sim$  up to 0.1-0.3
  - Fluid/kinetic pressure is dominant instability drive in high- $\beta$  ST plasmas

# Study 3 classes of IWM-unstable plasmas spanning low to high $\beta_N$

- Low  $\beta_N$  limit  $\sim 3.5$ , often saturated/long-lived mode
  - $q_{\min} \sim 2-3$
  - Common in early phase of current flat-top
  - Higher fraction of beam pressure, momentum (lower  $n_e$ )
- Intermediate  $\beta_N$  limit  $\sim 5$ 
  - $q_{\min} \sim 1.2-1.5$
  - Typical good-performance H-mode,  $H_{98} \sim 0.8-1.2$
- Highest  $\beta_N$  limit  $\sim 6-6.5$ 
  - $q_{\min} \sim 1$
  - “Enhanced Pedestal” H-mode  $\rightarrow$  high  $H_{98} \sim 1.5-1.6$
  - Broad pressure, rotation profiles, high edge rotation shear

# MARS-K: self-consistent linear resistive MHD including toroidal rotation and drift-kinetic effects

- Perturbed single-fluid linear MHD:**

*Y.Q. Liu, et al., Phys. Plasmas 15, 112503 2008*

$$(\gamma + in\Omega)\xi = \mathbf{v} + (\xi \cdot \nabla \Omega) R^2 \nabla \phi$$

$$\rho(\gamma + in\Omega)\mathbf{v} = \mathbf{j} \times \mathbf{B} + \mathbf{J} \times \mathbf{Q} - \nabla \cdot \mathbf{p}$$

$$+ \rho [2\Omega \hat{\mathbf{Z}} \times \mathbf{v} - (\mathbf{v} \cdot \nabla \Omega) R^2 \nabla \phi] - \nabla \cdot (\rho \xi) \Omega \hat{\mathbf{Z}} \times \mathbf{V}_0$$

$$(\gamma + in\Omega)\mathbf{Q} = \nabla \times (\mathbf{v} \times \mathbf{B}) + (\mathbf{Q} \cdot \nabla \Omega) R^2 \nabla \phi - \nabla \times (\eta \mathbf{j})$$

$$(\gamma + in\Omega)p = -\mathbf{v} \cdot \nabla P - \Gamma P \nabla \cdot \mathbf{v} \quad \mathbf{j} = \nabla \times \mathbf{Q}$$

- Rotation and rotation shear effects:**

- Mode-particle resonance operator:**

- Drift-kinetic effects in perturbed anisotropic pressure  $p$ :**

$$\mathbf{p} = p\mathbf{I} + p_{\parallel} \hat{\mathbf{b}}\hat{\mathbf{b}} + p_{\perp} (\mathbf{I} - \hat{\mathbf{b}}\hat{\mathbf{b}})$$

$$p_{\parallel} e^{-i\omega t + in\phi} = \sum_{e,i} \int d\Gamma M v_{\parallel}^2 f_L^1$$

$$p_{\perp} e^{-i\omega t + in\phi} = \sum_{e,i} \int d\Gamma \frac{1}{2} M v_{\perp}^2 f_L^1$$

$$f_L^1 = -f_{\epsilon}^0 \epsilon_k e^{-i\omega t + in\phi} \sum_{m,l,u} X_m^u H_{ml}^u \lambda_{ml} e^{-in\tilde{\phi}(t) + im\langle \dot{\chi} \rangle t + i l \omega_b t}$$

$$H_L = \frac{1}{\epsilon_k} [M v_{\parallel}^2 \vec{\kappa} \cdot \xi_{\perp} + \mu (Q_{L\parallel} + \nabla B \cdot \xi_{\perp})]$$

**Diamagnetic**

$$\lambda_{ml} = \frac{n[\omega_{*N} + (\hat{\epsilon}_k - 3/2)\omega_{*T} + \omega_E] - \omega}{n(\underbrace{\langle \omega_d \rangle}_{\text{Precession}} + \underbrace{\omega_E}_{\text{ExB}}) + [\underbrace{\alpha(m + nq)}_{\text{Transit and bounce}} + l]\omega_b - i \underbrace{\nu_{\text{eff}}}_{\text{Collisions}} - \omega}$$

- Fast ions: analytic slowing-down  $f(v)$  model – isotropic or anisotropic**

**This talk**

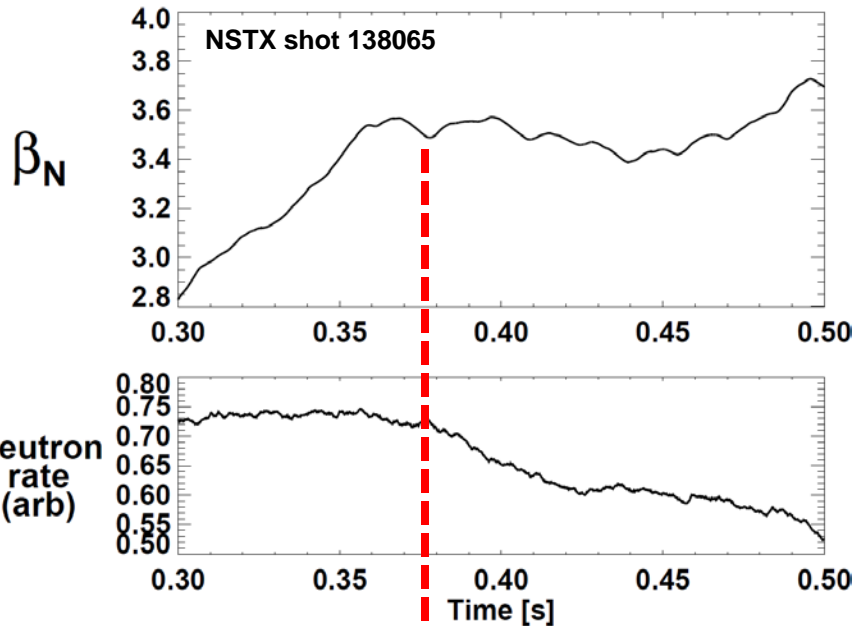
- Include toroidal flow only:  $\mathbf{v}_{\phi} = R\Omega_{\phi}(\psi)$  and  $\omega_E = \omega_E(\psi)$**

# Study 3 classes of IWM-unstable plasmas spanning low to high $\beta_N$

- **Low  $\beta_N$  limit  $\sim 3.5$** , often saturated/long-lived
  - $q_{\min} \sim 2-3$
  - Common in early phase of current flat-top
  - Higher fraction of beam pressure, momentum (lower  $n_e$ )
- Intermediate  $\beta_N$  limit  $\sim 5$ 
  - $q_{\min} \sim 1.2-1.5$
  - Typical good-performance H-mode,  $H_{98} \sim 0.8-1.2$
- Highest  $\beta_N$  limit  $\sim 6-6.5$ 
  - $q_{\min} \sim 1$
  - “Enhanced Pedestal” H-mode  $\rightarrow$  high  $H_{98} \sim 1.5-1.6$
  - Broad pressure, rotation profiles, high edge rotation shear

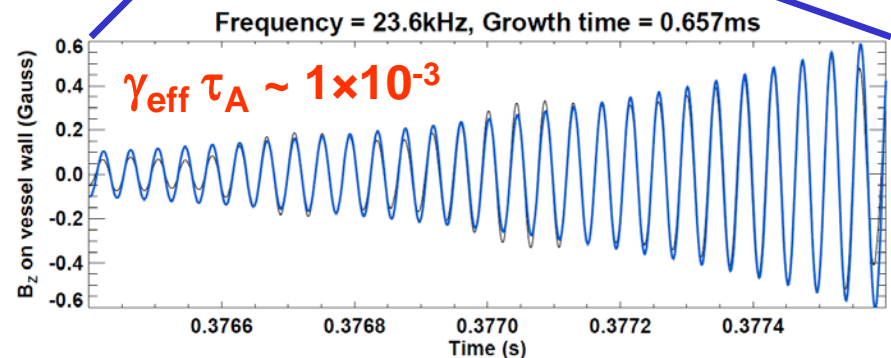
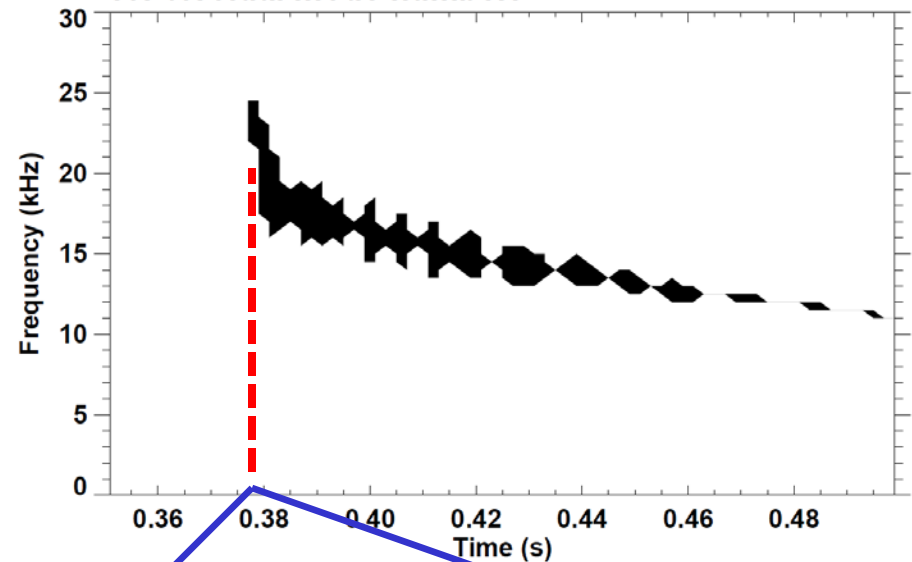
# Saturated $f=15\text{-}30\text{kHz}$ $n=1$ mode common during early $I_p$ flat-top phase

Fixed  $P_{\text{NBI}} = 3\text{MW}$ ,  $I_p = 800\text{kA}$ ,  $\beta_T = 10\text{-}15\%$



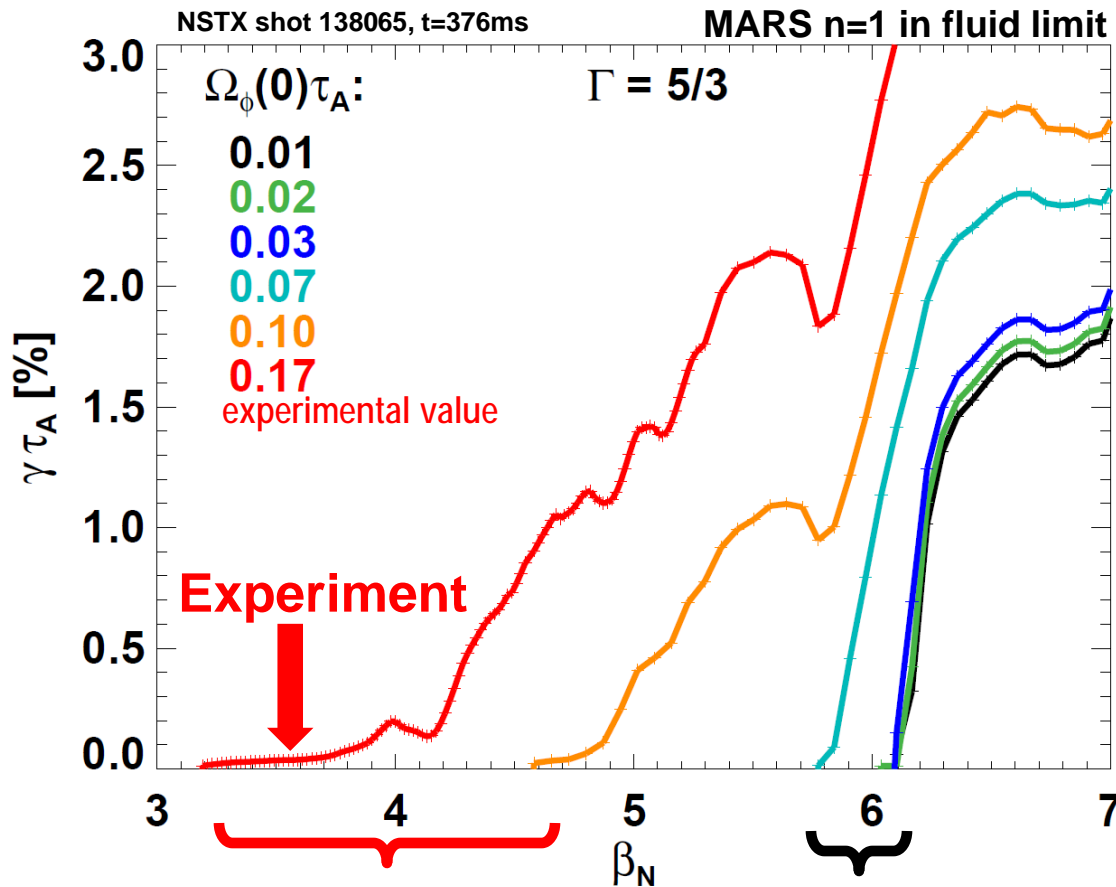
**Mode clamps  $\beta_N$  to  $\sim 3.5$ ,  
reduces neutron rate  $\sim 20\%$**   
sometimes slows  $\rightarrow$  locks  $\rightarrow$  disrupts

Shot 138065  $\omega B(\omega)$  spectrum  
for toroidal mode number:





# Fluid (non-kinetic) MARS-K calculations find: Rotation reduces IWL $\beta_N = 6 \rightarrow 3-3.5$



High rotation  $\beta_N$  limit  $\sim 4.5 \rightarrow 3.2$   
for  $\Omega_\phi(0)\tau_A = 10 \rightarrow 17\%$  (experimental)

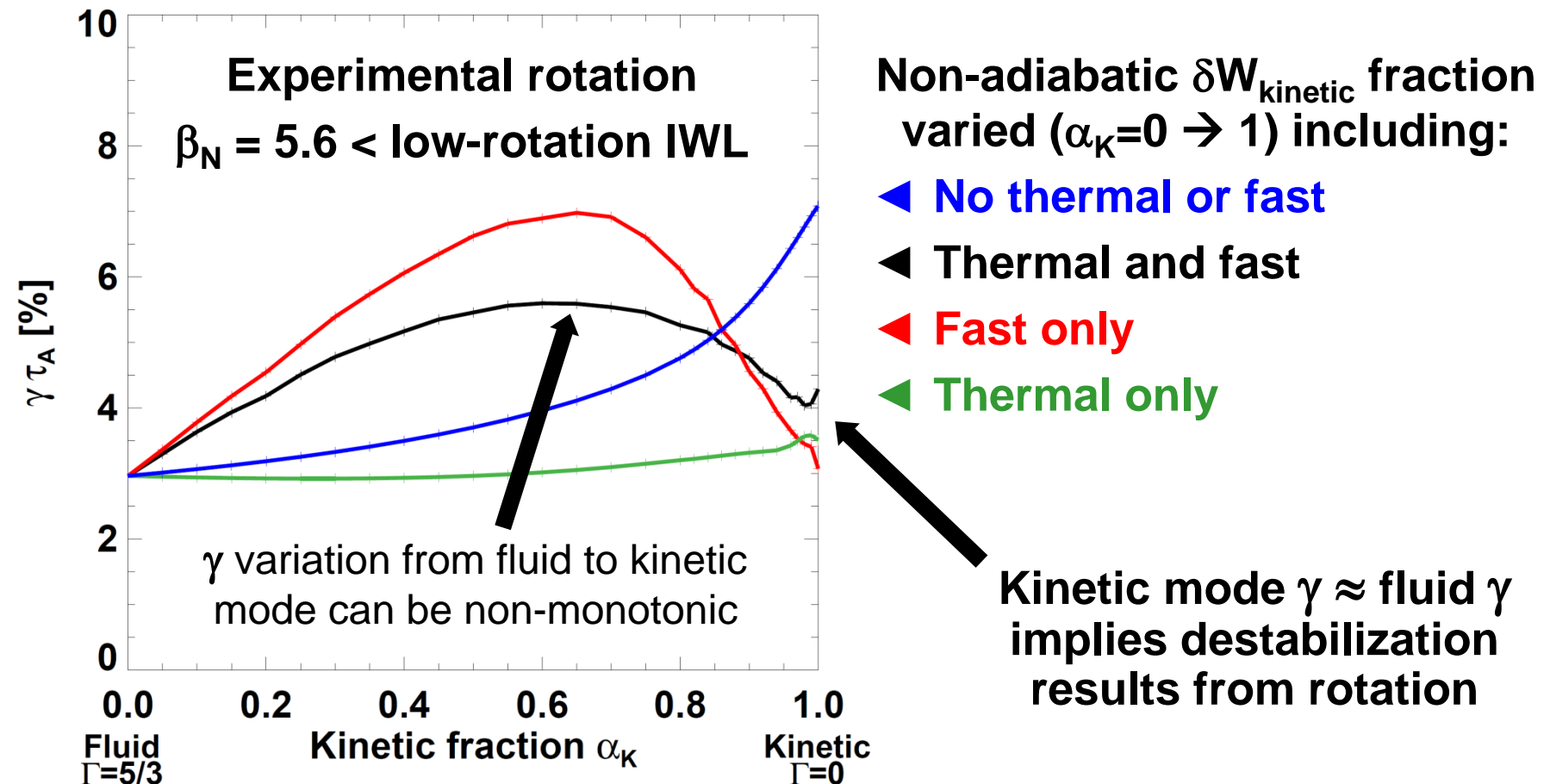
Low rotation  $\beta_N$  limit  $\sim 6$   
for  $\Omega_\phi(0)\tau_A = 1 \rightarrow 7\%$

Fluid MARS marginal  $\beta_N \sim 3 - 4$  consistent with experiment



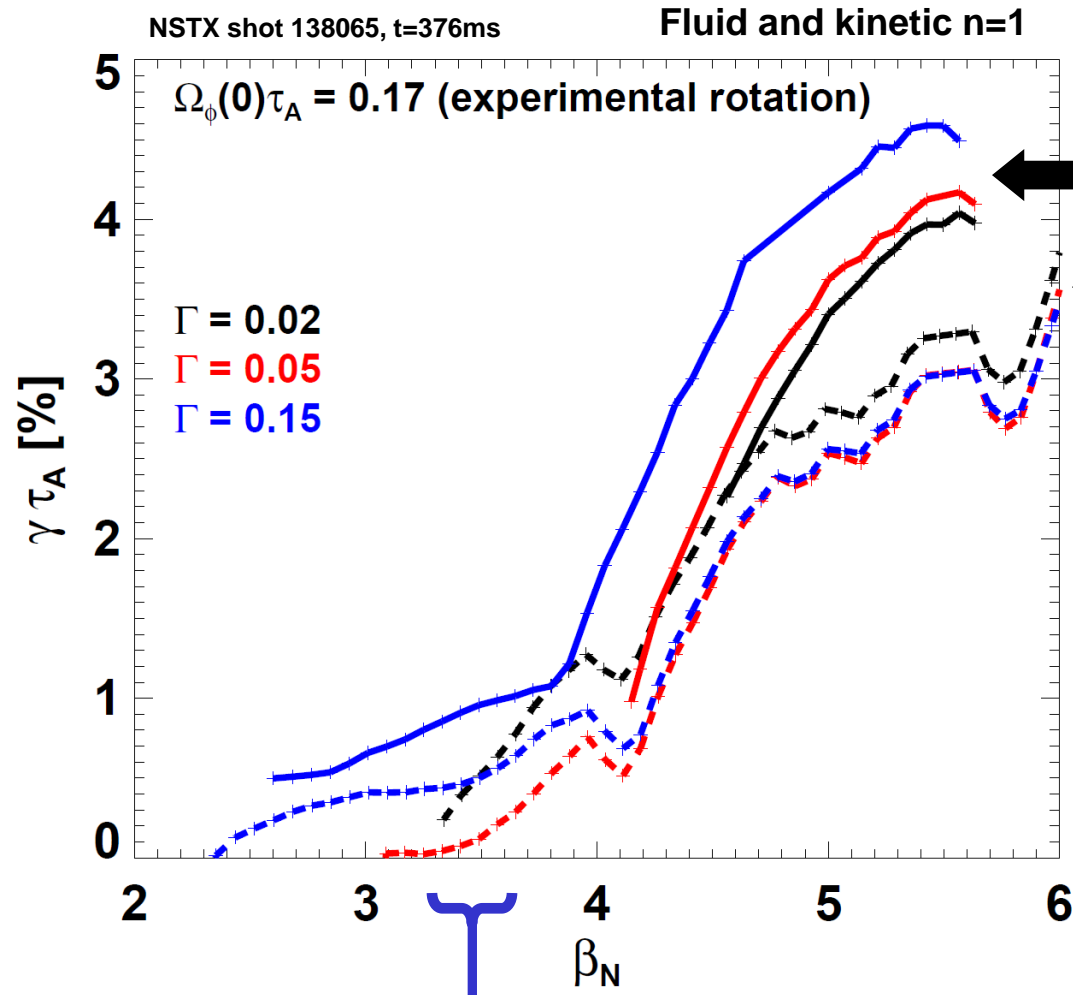
# Kinetic mode also destabilized by rotation

Kinetic mode tracked numerically by starting from fluid root and increasing kinetic fraction  $\alpha_K = 0 \rightarrow 1$  as  $\Gamma = 5/3 \rightarrow 0$



# Kinetic stability limit similar to fluid limit:

Marginal  $\beta_N < 3.5$  far below low-rotation  $\beta_N$  limit of  $\sim 6$



Solid: Kinetic  $\gamma$

Dashed: Fluid  $\gamma$

## Convergence issues:

- Drift-kinetic MHD model assumes fluid  $\Gamma = 0$
- When  $\Gamma = 0$ , MARS can sometimes track wrong root or find spurious root
- **Solution:** take  $\Gamma \rightarrow 0$  limit, monitor eigenfunctions for continuous trend vs.  $\alpha_k, \beta, \Gamma$

Experimental  $\beta_N$  for  $n=1$  mode onset

# Real part of complex energy functional consistent with rotational destabilization ( $\delta W_{\text{rot}} \leq 0$ ) across minor radius

$$\delta K + \delta W = 0 \quad (\gamma^{re})^2 = (\delta W_K^{re} + \delta W_F^{re} + \delta W_{vb} + \delta W_{rot}^{re}) / \delta K_1 \quad \delta K_1 = -\frac{1}{2} \int d^3x \rho |\vec{\xi}_\perp|^2 < 0$$

$$\delta W_{rot} = \delta W_\Omega + \delta W_{d\Omega} + \delta W_{cf} + \delta K_2$$

**Coriolis -  $\Omega$**

$$\delta W_\Omega = \frac{1}{2} \int d^3x \left[ -2\rho\Omega(\gamma + in\Omega) \mathbf{Z} \times \vec{\xi}_1 \cdot \vec{\xi}_\perp^* \right]$$

**Coriolis -  $d\Omega/d\rho$**

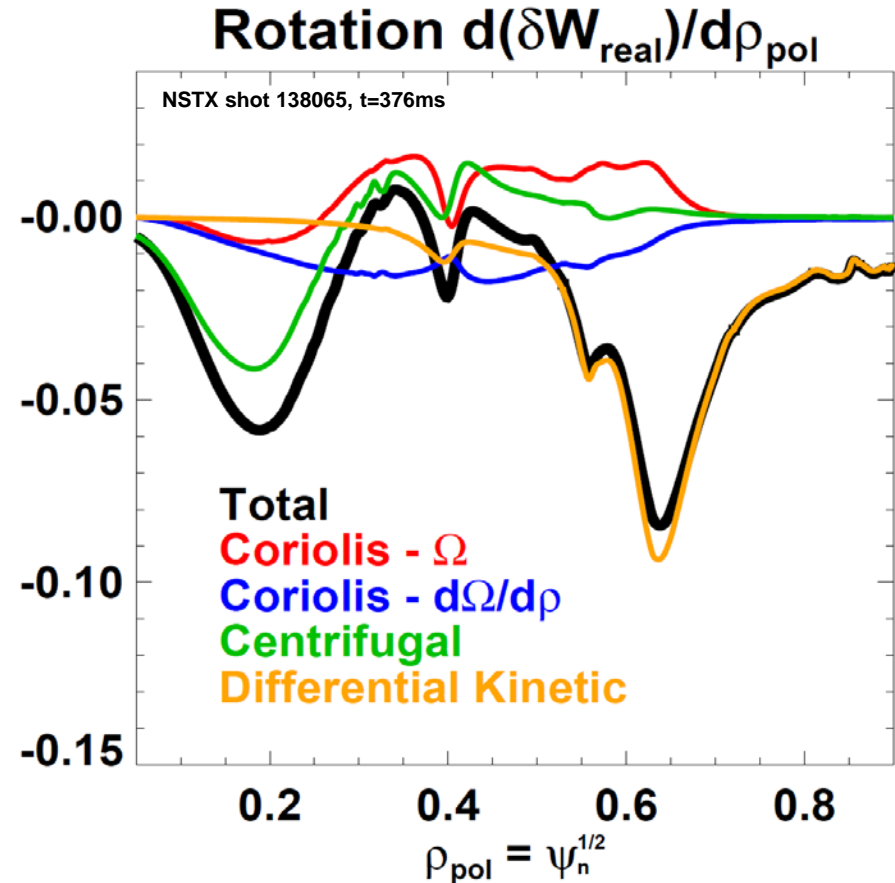
$$\delta W_{d\Omega} = \frac{1}{2} \int d^3x R \left( 2\rho\Omega(\vec{\xi}_1 \cdot \nabla\Omega) \vec{\xi}_{\perp R}^* \right)$$

**Centrifugal**

$$\delta W_{cf} = \frac{1}{2} \int d^3x R \Omega^2 \nabla \cdot (\rho \vec{\xi}_1) \vec{\xi}_{\perp R}^*$$

**Differential kinetic (always destabilizing)**

$$\delta K_2 = -\frac{1}{2} \int d^3x \rho (\omega - n\Omega)^2 |\vec{\xi}_\perp|^2$$



Destabilization from: Coriolis ( $d\Omega/d\rho$ ), centrifugal, differential kinetic

# Analytic model of rotational-shear destabilization is being compared to MARS results and experiment

**Model: low rotation, high rotation shear** (Ming Chu, Phys. Plasmas, Vol. 5, No. 1, (1998) 183)

## 1. Ideal interchange criterion including rotation shear:

$$D_{I,\Omega} = D_I + \frac{1}{4} (M_a^2 + A) + \frac{\beta_\Gamma M_s^2}{F(\beta_\Gamma - M_s^2)} \times \left[ D_I + \frac{1}{2} \left( \frac{1}{2} - H \right) \right]^2 > 0$$

↑  
Ideal interchange index w/o rotation  
Glasser, Greene, Johnson – Phys. Fluids (1975) 875

β<sub>Γ</sub> = compressional Alfvén wave β

## 2. Kelvin-Helmholtz criterion:

$$M_s^2 > \beta_\Gamma$$

$$\beta_\Gamma = \frac{\Gamma p}{\Gamma p + p'^2 (\langle B^2 / |\nabla V|^2 \rangle / \Lambda^2 F)}$$

M<sub>a</sub> = (shear) Alfvén wave excitation Mach number

$$M_a^2 = \frac{1}{\Lambda^2} \left( \frac{\partial \Omega}{\partial V} \right)^2 \frac{\rho M \chi'^2}{(2\pi)^2}$$

M<sub>s</sub> = sound Alfvén wave excitation Mach number

$$M_s^2 = \frac{\chi'^2 (\partial \Omega / \partial V)^2 \langle B^2 \rangle \rho F}{p'^2 \langle B^2 / |\nabla V|^2 \rangle (2\pi)^2}$$

Rotation shear

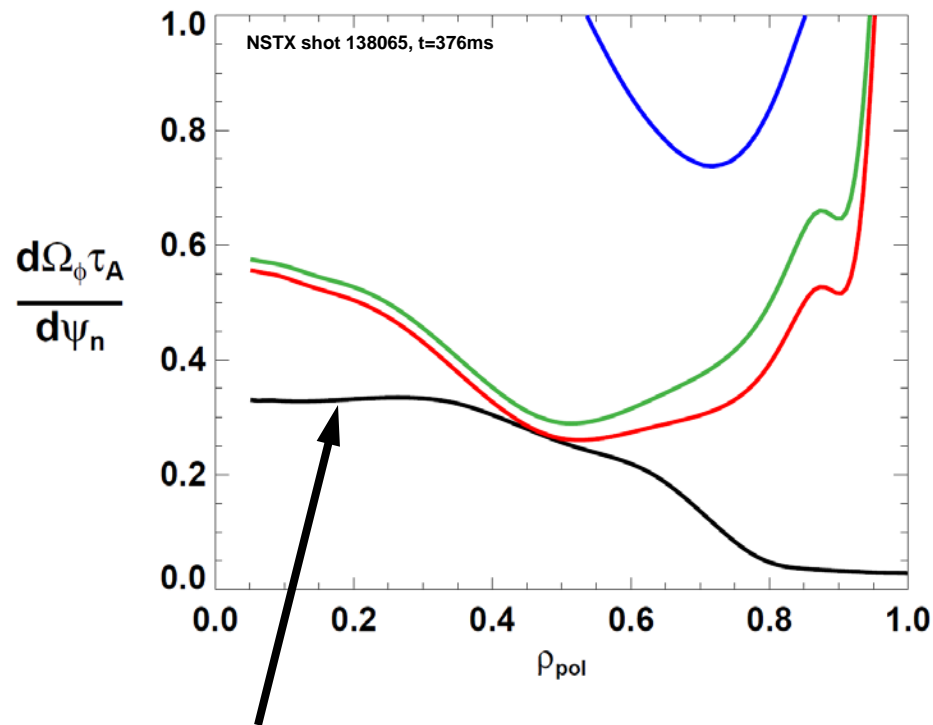
**destabilizes Alfvén wave directly or through sound wave coupling**

# Experiment marginally stable to rotation-driven interchange/Kelvin-Helmholtz near half-radius

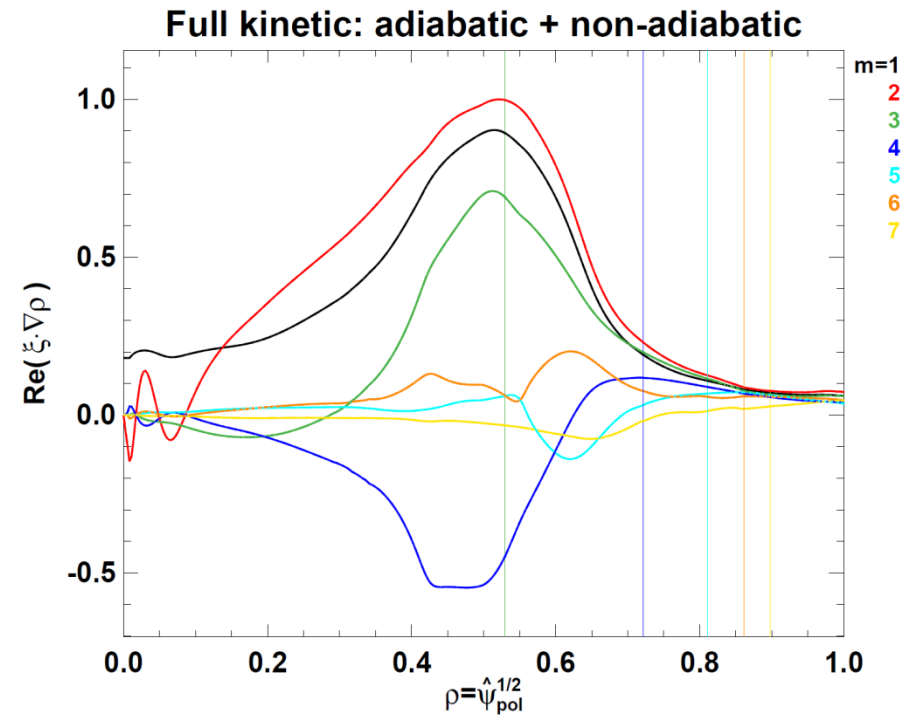
Chu model marginal  $\Omega'$  profiles:

$$D_{I,\Omega} = 0 \quad M_s^2 = \beta_\Gamma \quad D_{I,\Omega}(\Gamma=0) = 0$$

$\nabla p$  dominant    KH dominant



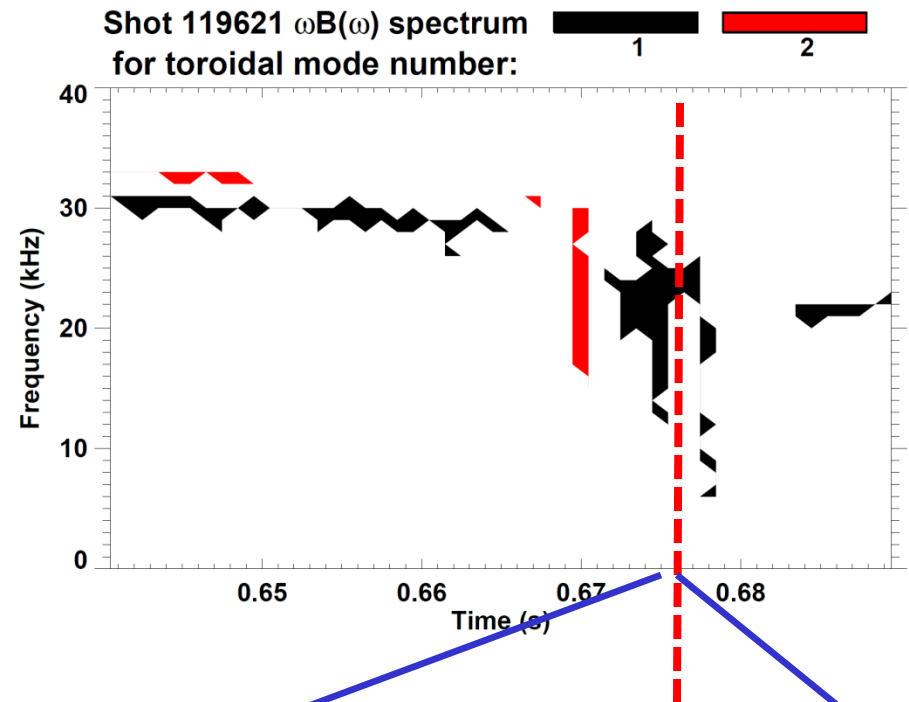
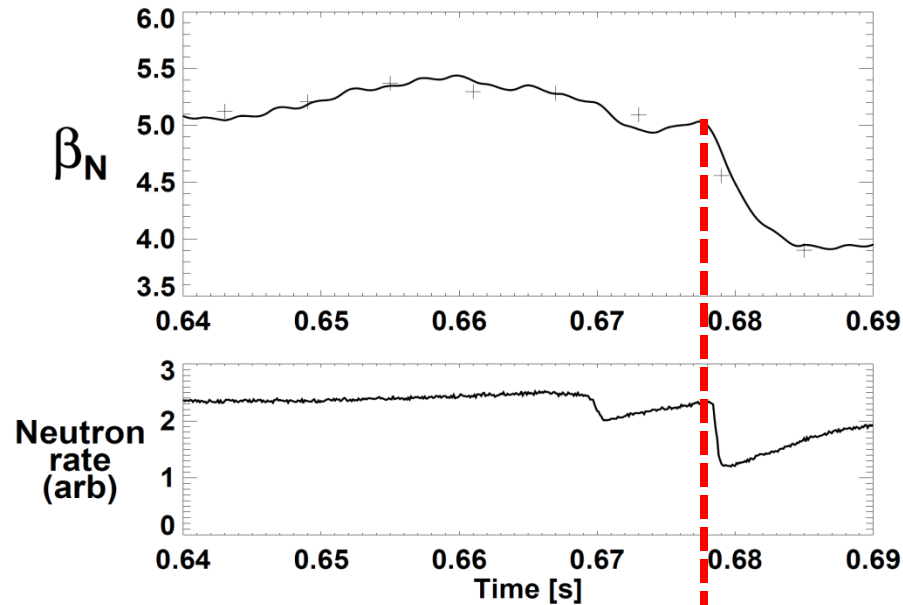
MARS full kinetic eigenfunction displacement largest near  $r/a \sim 0.5$



# Study 3 classes of IWM-unstable plasmas spanning low to high $\beta_N$

- Low  $\beta_N$  limit  $\sim 3.5$ , often saturated/long-lived
  - $q_{\min} \sim 2-3$
  - Common in early phase of current flat-top
  - Higher fraction of beam pressure, momentum (lower  $n_e$ )
- **Intermediate  $\beta_N$  limit  $\sim 5$** 
  - $q_{\min} \sim 1.2-1.5$
  - Typical good-performance H-mode,  $H_{98} \sim 0.8-1.2$
- Highest  $\beta_N$  limit  $\sim 6-6.5$ 
  - $q_{\min} \sim 1$
  - “Enhanced Pedestal” H-mode  $\rightarrow$  high  $H_{98} \sim 1.5-1.6$
  - Broad pressure, rotation profiles, high edge rotation shear

# Small $f=30\text{kHz}$ continuous $n=1$ mode precedes larger 20-25kHz $n=1$ bursts

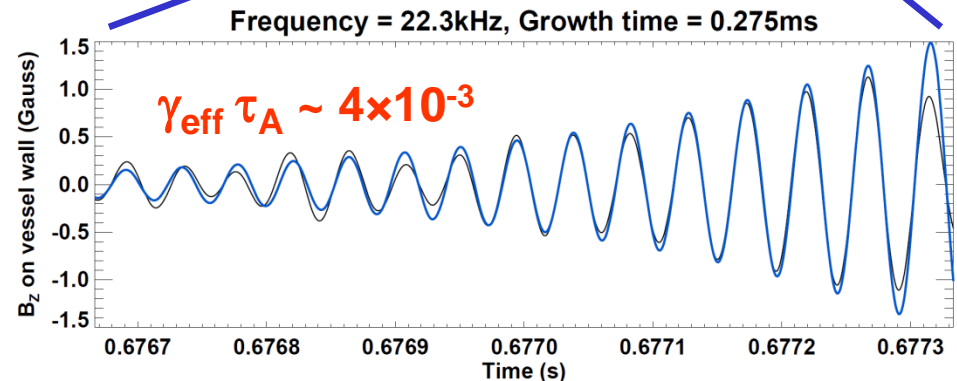


First large  $n=1$  burst  $\rightarrow$

20% drop in  $\beta_N$

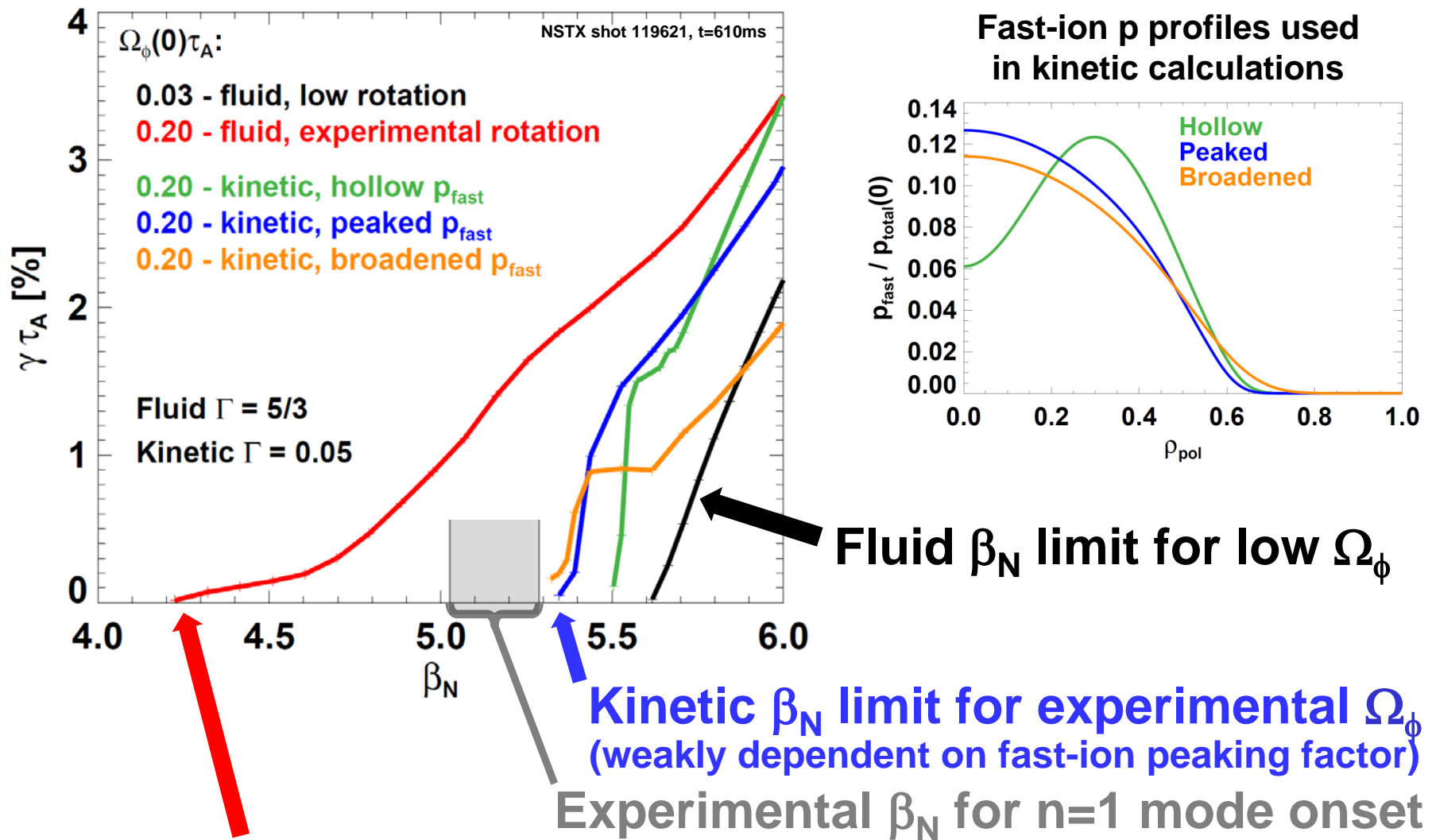
50% neutron rate drop

Later  $n=1$  modes  $\rightarrow$  full disruption



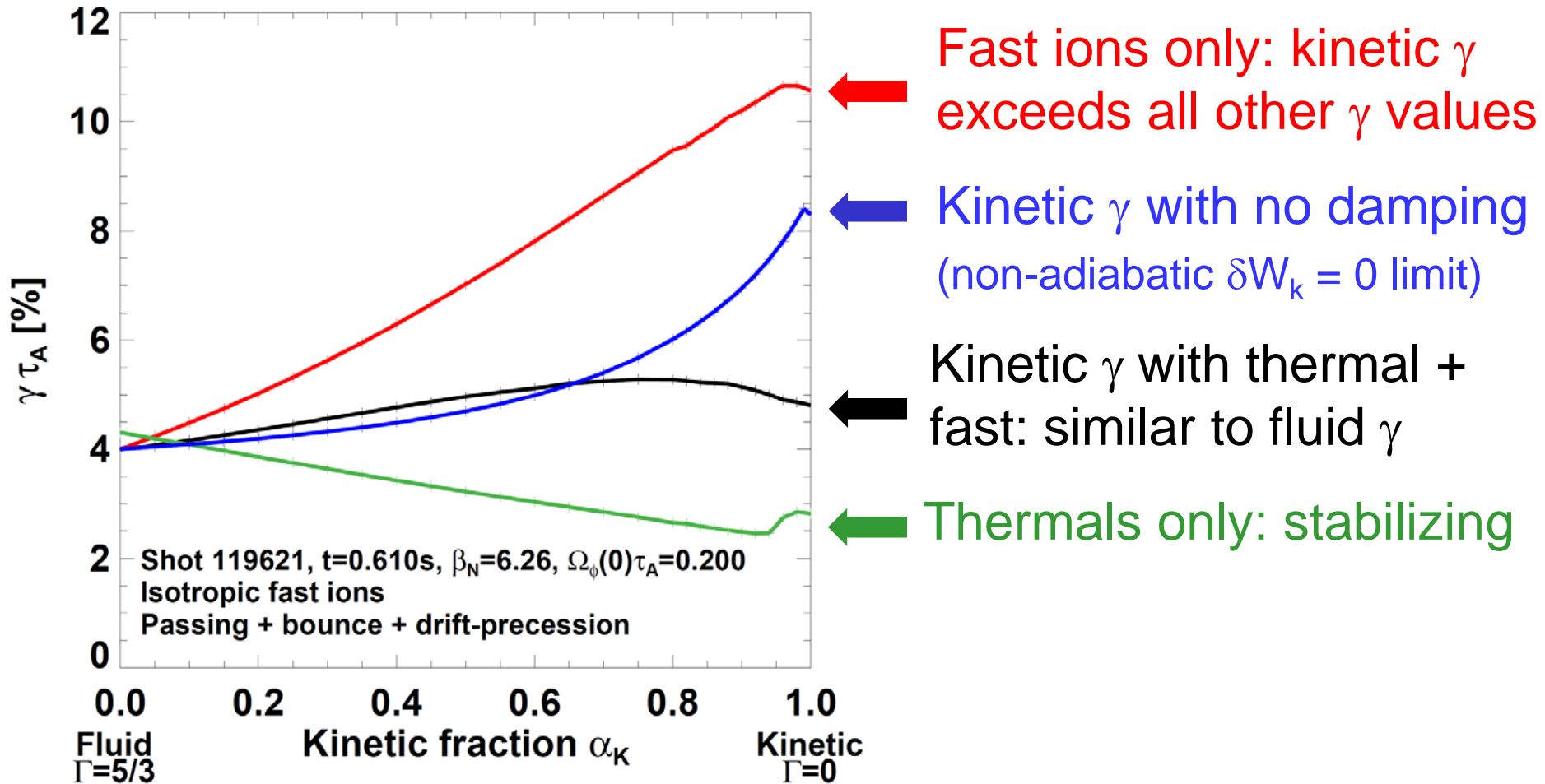


# Kinetic $\beta_N$ limit consistent with experiment, fluid calculation under-predicts experimental limit



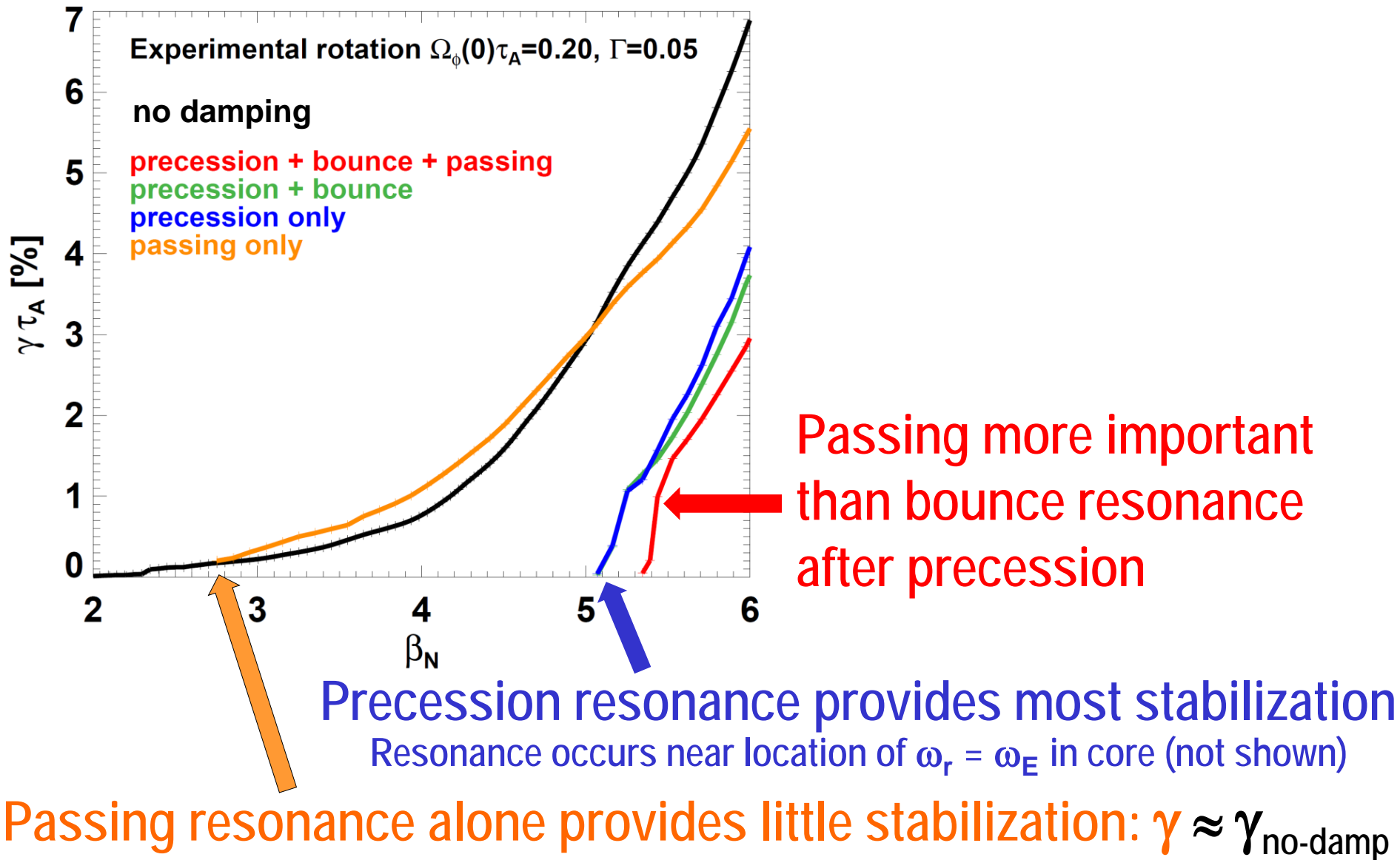
Fluid  $\beta_N$  limit for experimental  $\Omega_\phi$  ( $\Delta\beta_N = -1.4$  vs. low rotation)

# Kinetic fast-ions destabilizing, thermals stabilizing



Implication: thermal damping stabilizes rotation-driven mode

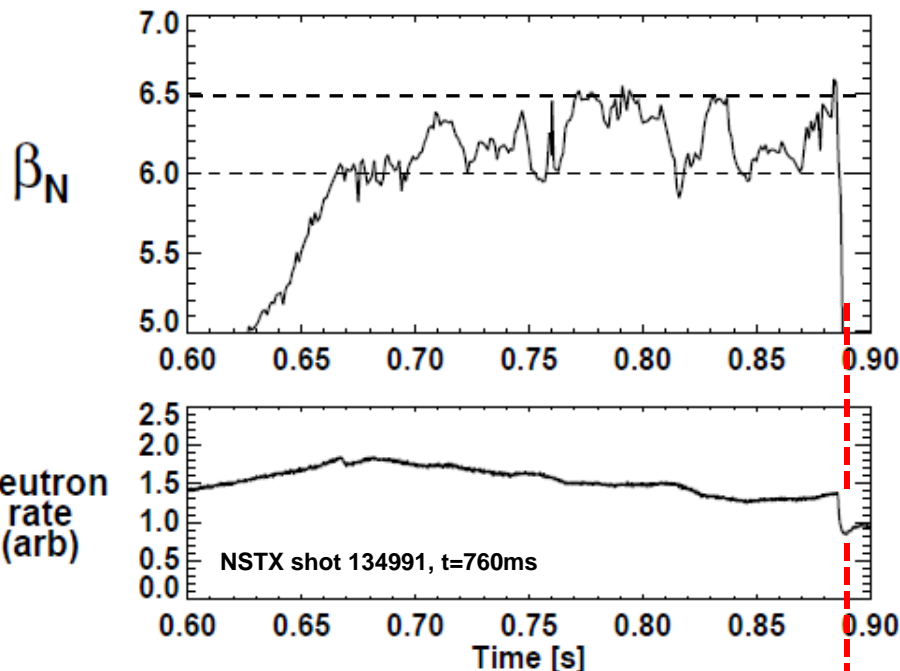
# Precession resonance dominates damping, highest $\beta_N$ requires inclusion of passing resonance



# Study 3 classes of IWM-unstable plasmas spanning low to high $\beta_N$

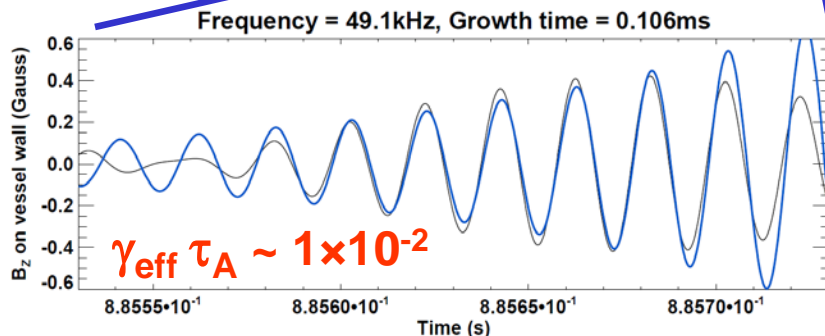
- Low  $\beta_N$  limit  $\sim 3.5$ , often saturated/long-lived
  - $q_{\min} \sim 2-3$
  - Common in early phase of current flat-top
  - Higher fraction of beam pressure, momentum (lower  $n_e$ )
- Intermediate  $\beta_N$  limit  $\sim 5$ 
  - $q_{\min} \sim 1.2-1.5$
  - Typical good-performance H-mode,  $H_{98} \sim 0.8-1.2$
- **Highest  $\beta_N$  limit  $\sim 6-6.5$** 
  - $q_{\min} \sim 1$
  - “Enhanced Pedestal” H-mode  $\rightarrow$  high  $H_{98} \sim 1.5-1.6$
  - Broad pressure, rotation profiles, high edge rotation shear

# Experimental characteristics of highest- $\beta_N$ MHD



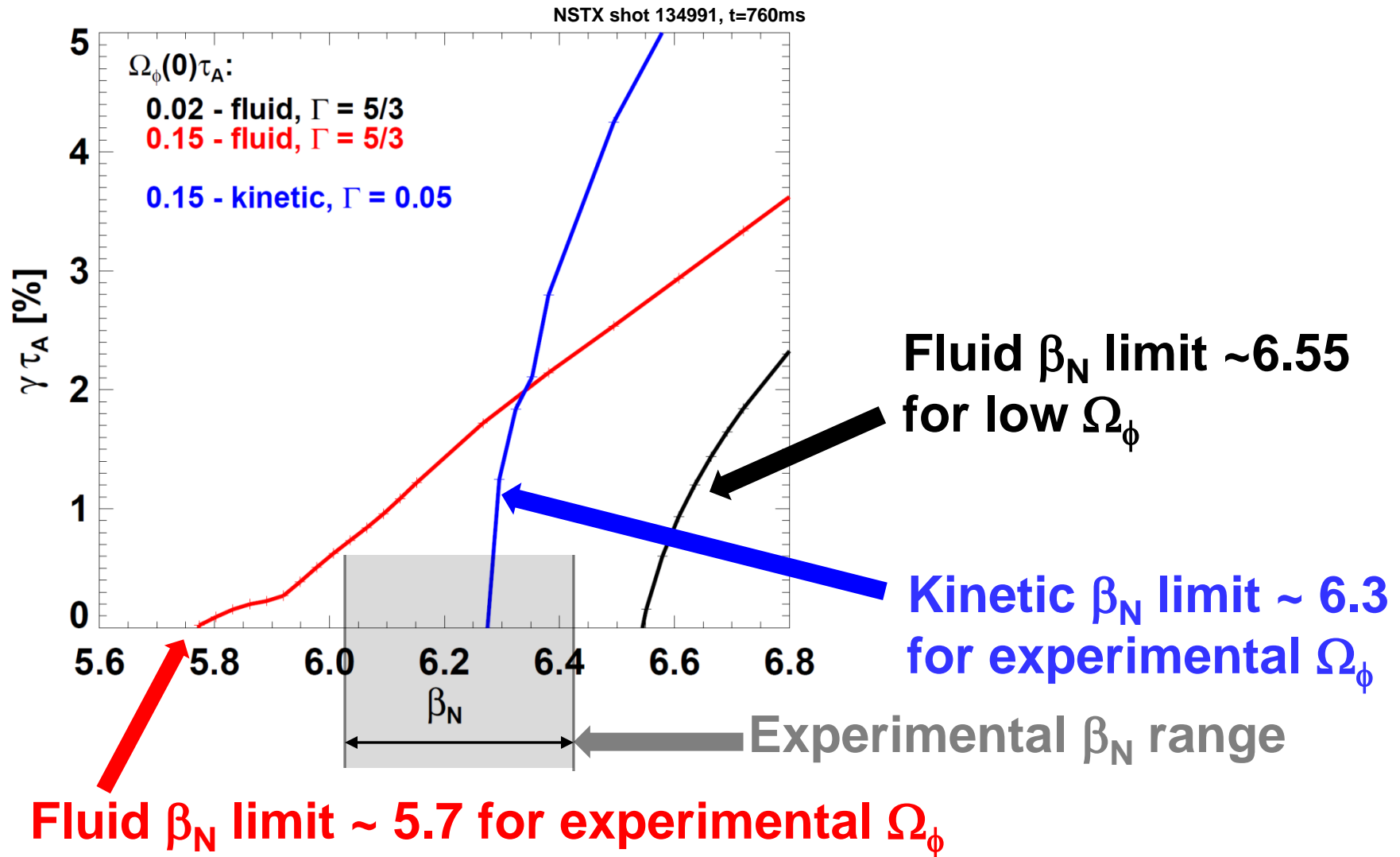
- $\beta_N = 6-6.5$  sustained for  $2-3\tau_E$ 
  - Oscillations from ELMs and bottom/limiter interactions
  - Possible small RWM activity
  - Only small core MHD (steady neutron rate)

- $f = 50\text{kHz}$  mode causes 35%  $\beta_N$  drop ending high- $\beta$  phase
  - Mode grows very fast ( $\sim 100\mu\text{s}$ )
  - n-number difficult to determine
  - Possible that mode has  $n > 1$



# Kinetic $n=1$ stability consistent with access to $\beta_N > 6$

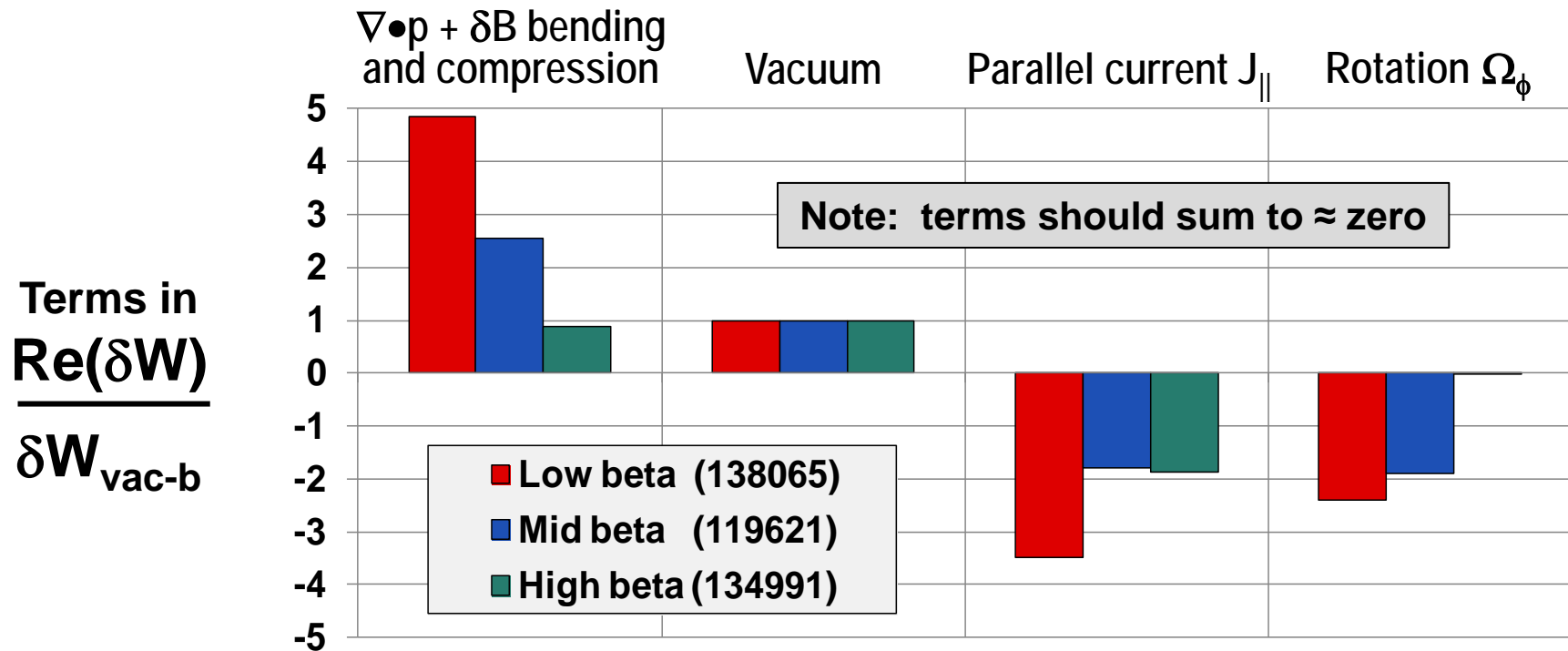
## Fluid calculation under-predicts experimental $\beta_N$



Rotational de-stabilization weaker ( $\Delta\beta_N = -0.8$  vs. low rotation)

# Energy analysis near marginal stability elucidates trends from growth-rate scans

- All cases: field-line bending+compression balances primarily  $\nabla p$



- Low  $\beta$ :  $J_{||}$  (low  $q$  shear) and high  $\Omega_{\phi}$  strongly destabilizing
- Mid  $\beta$ : Reduced destabilization from  $J_{||}$  &  $\Omega_{\phi}$  increases  $\beta$  limit
- High  $\beta$ : Large  $\Omega_{\phi}'$  at edge minimizes  $\Omega_{\phi}$  drive  $\rightarrow$  highest  $\beta$



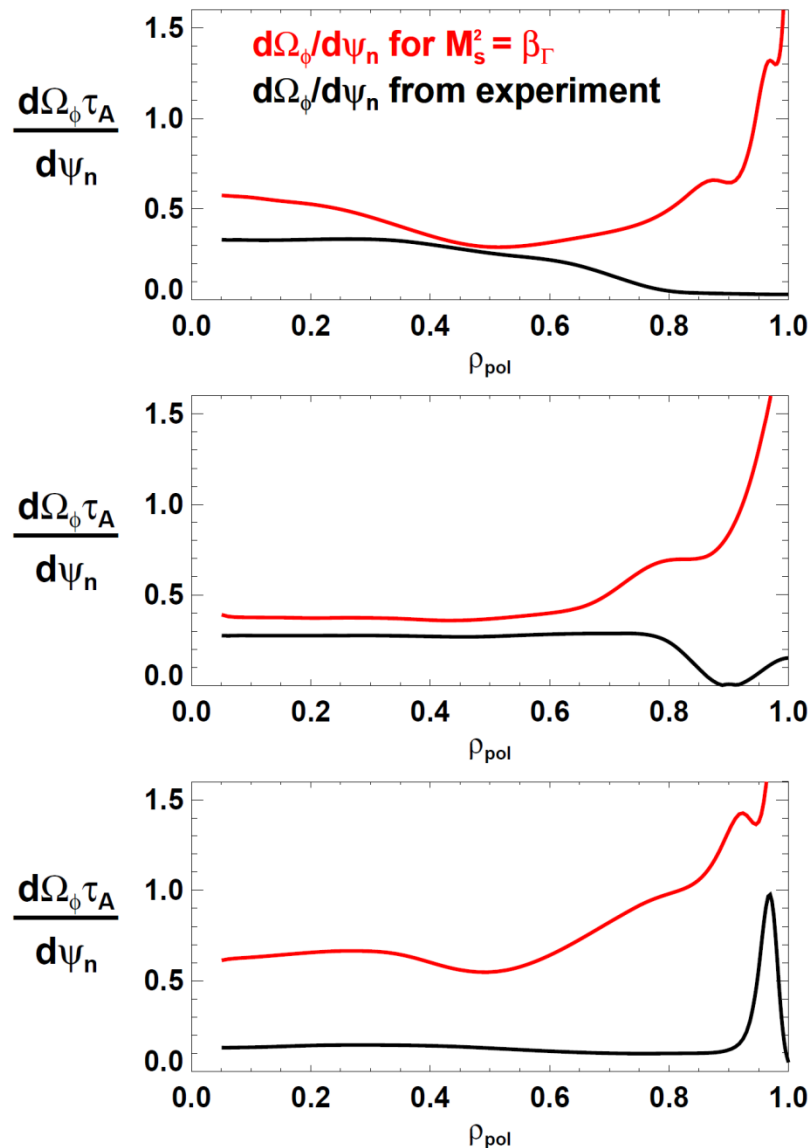
# Summary

- Rotation, kinetic effects can modify ideal-wall limit at high  $\Omega_\phi$ ,  $\beta$
- Rotation effects most pronounced for plasmas near rotation-shear enhanced interchange/Kelvin-Helmholtz (KH) threshold
  - High rotation shear near edge is most stable in theory and experiment
- Kinetic damping from thermal resonances can be sufficient to suppress rotation-driven mode  $\rightarrow$  access low-rotation IWL
- Kinetic  $\beta$  limits generally closer to experiment than fluid limits
- Future work:
  - Understand kinetic damping of rotation-driven modes in more detail
  - Test more realistic fast-ion distribution functions – anisotropic / TRANSP
  - Assess finite orbit width effects (see next talk) – for fast, edge thermal ions
  - Assess modifications to RWM stability from rotation/rotation shear
  - Utilize off-axis NBI, 3D  $\delta B$ /NTV in NSTX-U to explore IWL limit vs. rotation

# Backup

---

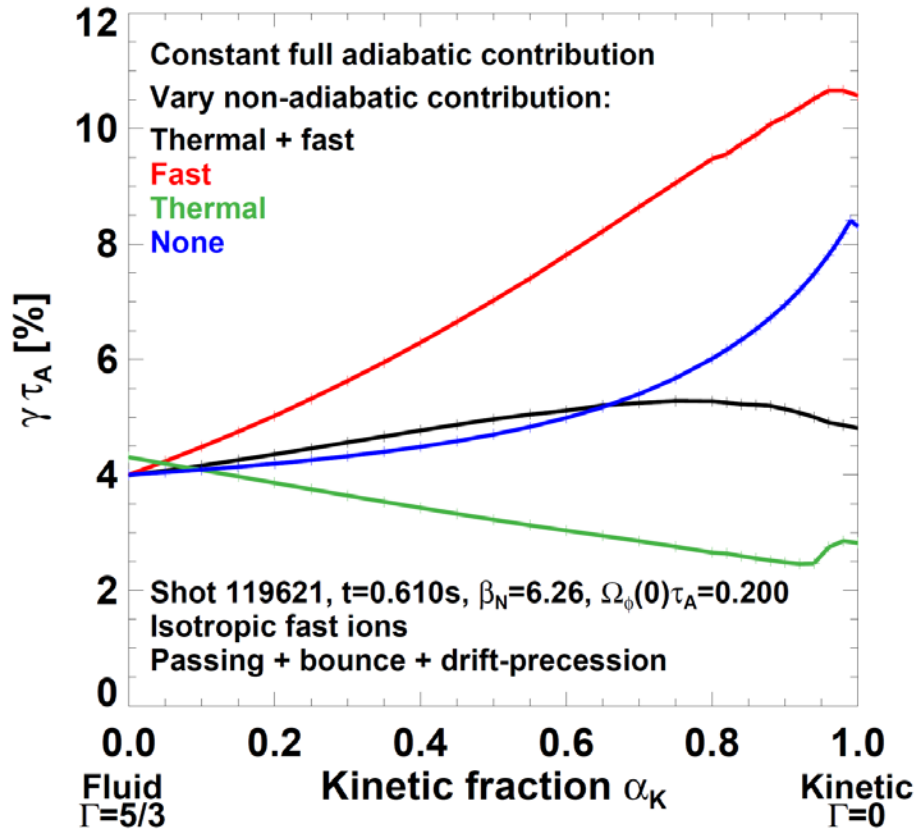
# Comparison of cases for KH marginal rotation shear



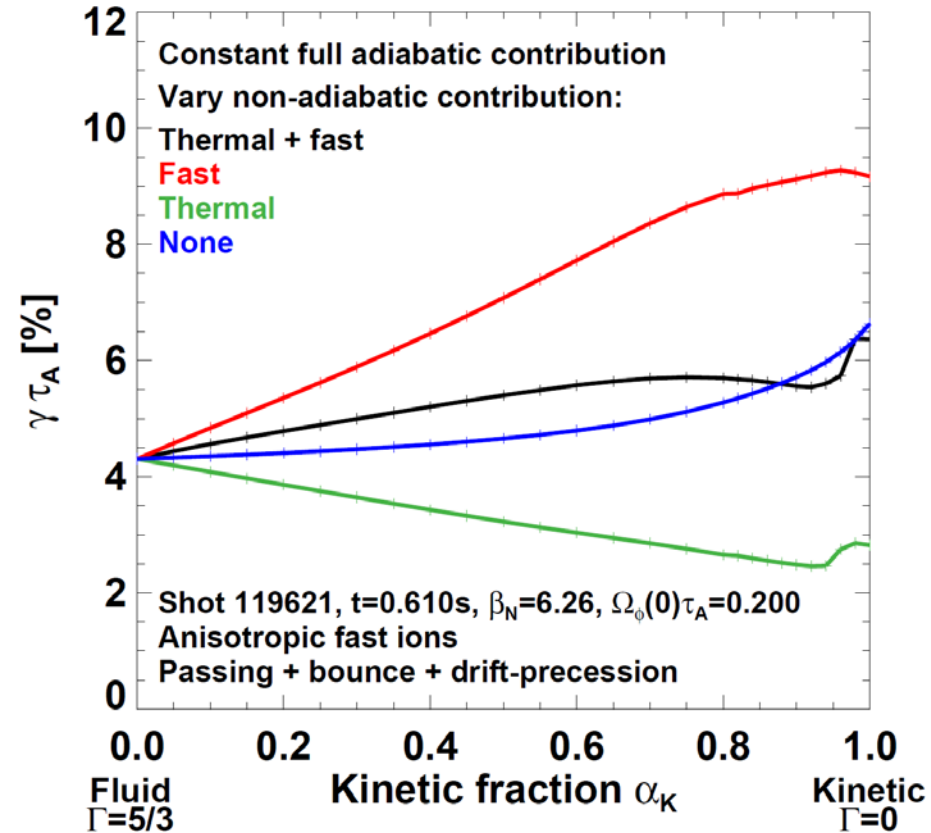
- Low  $\beta$  case
  - Rotation shear mode not stabilized kinetically
- Medium  $\beta$  case
  - Nearly achieve no-rotation IWL via kinetic stabilization
- High  $\beta$  case
  - High edge rotation shear stabilizing – minimizes needed kinetic stabilization

# Initial studies find anisotropic fast-ion distribution has damping vs. $\alpha_k$ , $\Gamma$ trends similar to isotropic

## Isotropic



## Anisotropic



Anisotropic fast-ion passing resonance can cause  $\delta W_k$  singularities – investigating...

# Inclusion of thermal and fast-ions (TRANSP) in total pressure can significantly modify pressure profile shape

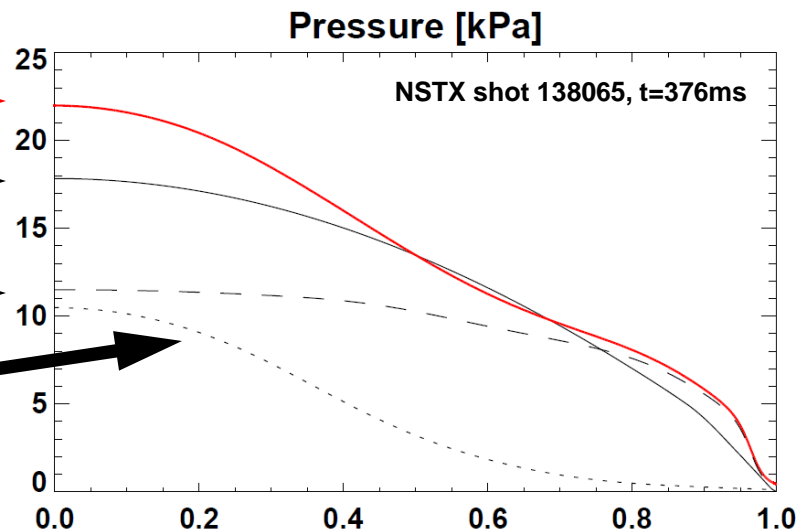
**Total pressure (thermal + fast)** →

**Reconstruction** →

(without kinetic pressure constraint)

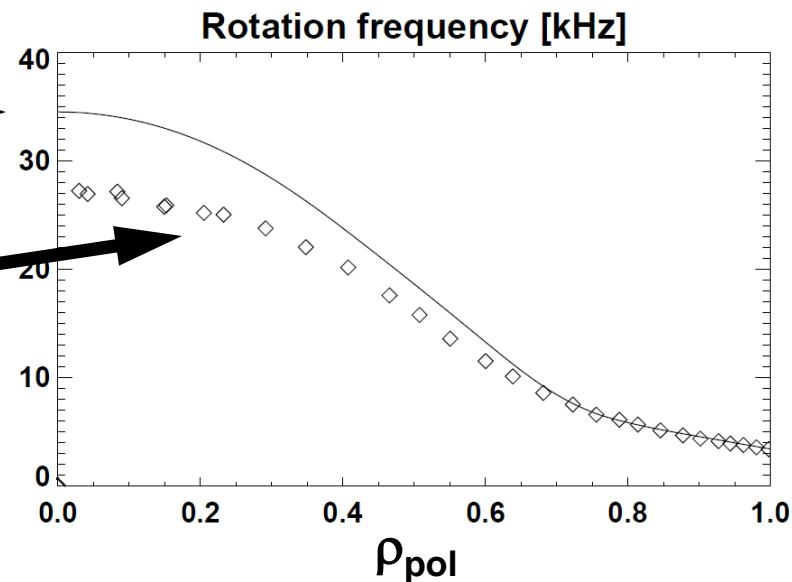
**Thermal** →

**Fast** →



**Thermal + NBI** →  
(includes fast-ion angular momentum)

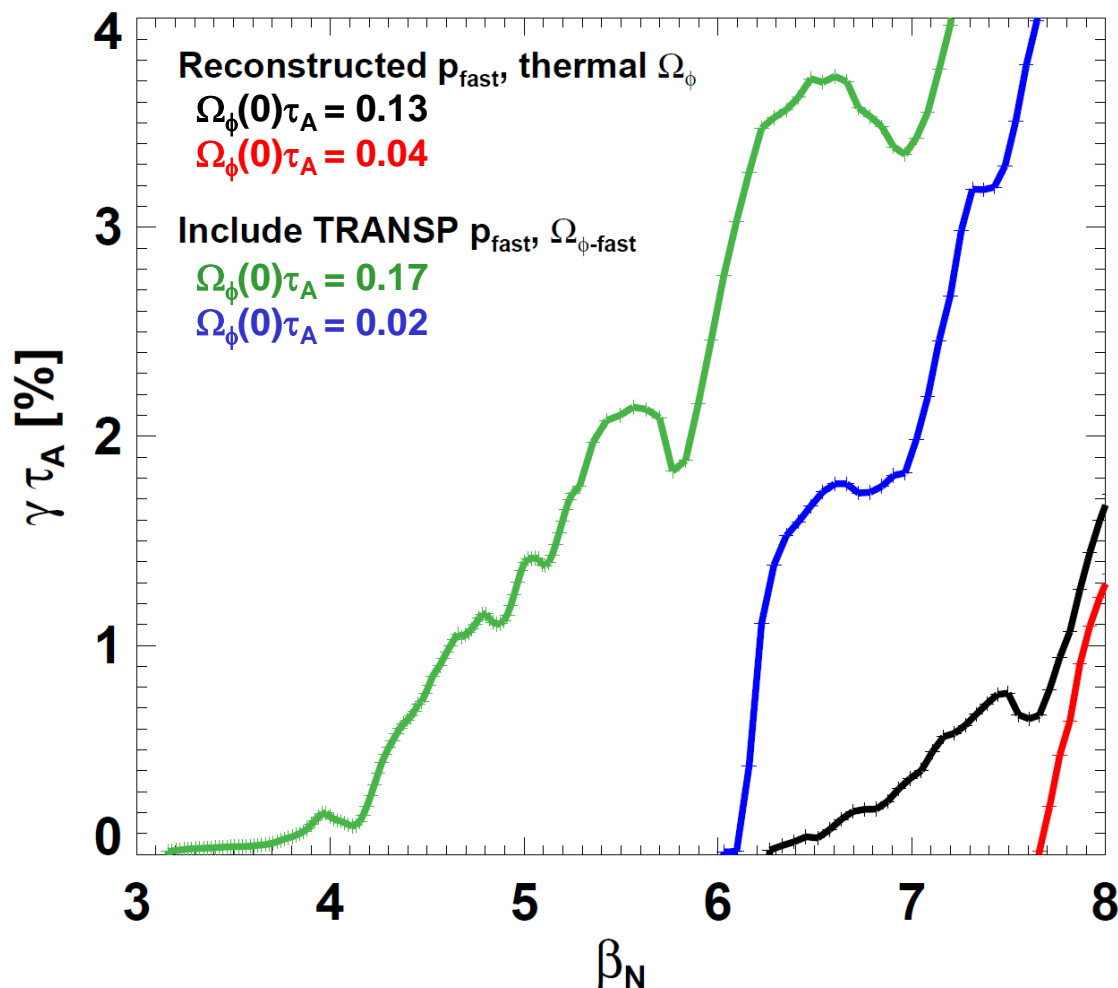
**Thermal ( $C^{6+}$ )** →



# Inclusion of fast-ion pressure and angular momentum (computed from TRANSP) significantly lowers marginal $\beta_N$

NSTX shot 138065,  $t=376\text{ms}$

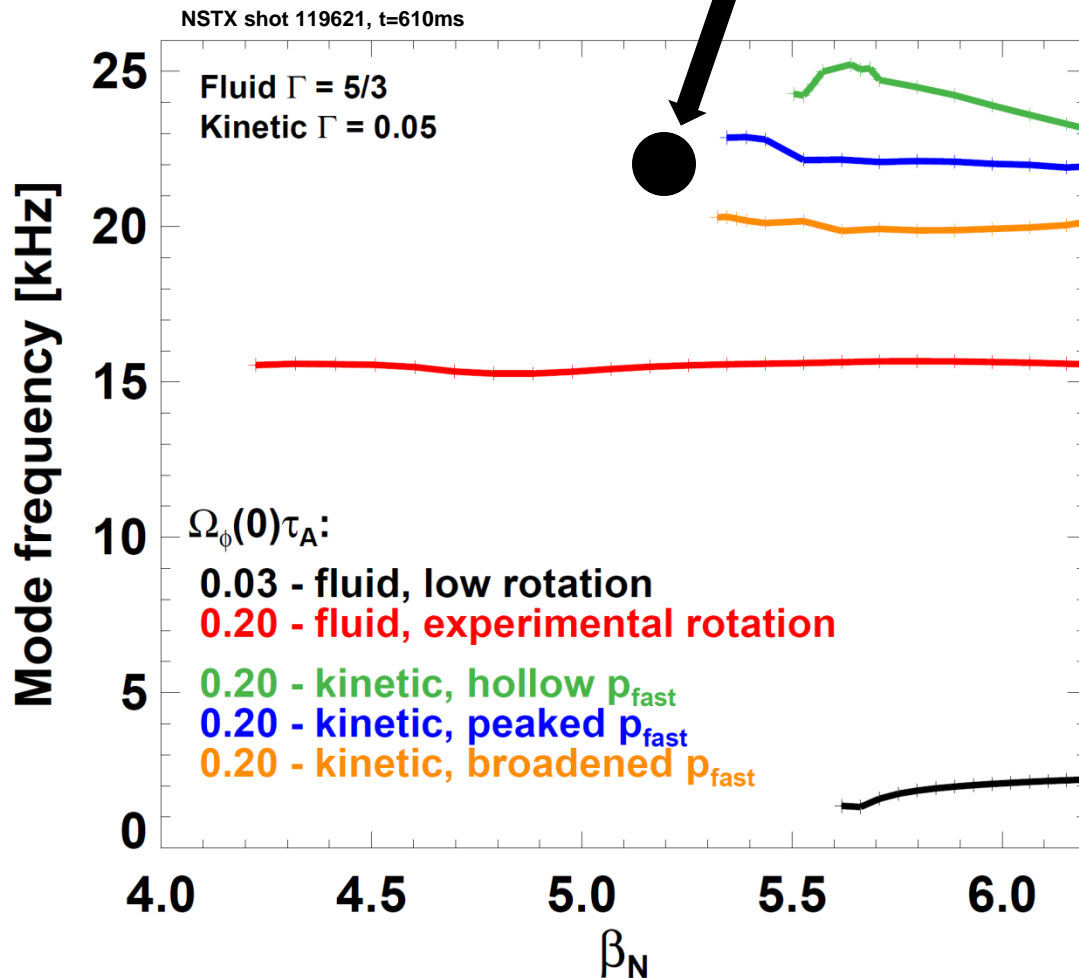
## FLUID CALCULATIONS



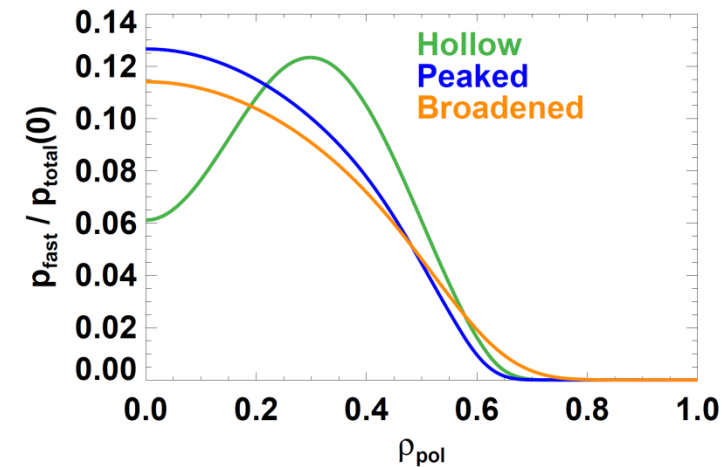
- Increased pressure profile peaking from fast-ions lowers  $\beta_N$  limit from **7.7** to **6.1** at low rotation
- Effective  $\beta_N$  limit at experimental rotation reduced from **6.3** to **~3.4**

# Measured mode frequency more consistent with kinetic calculation

## Measured mode frequency



## Fast-ion $p$ profiles used in kinetic calculations





# Real part of complex energy functional provides equation for growth-rate useful for understanding instability sources

## Dispersion relation

$$\delta K + \delta W = 0$$

## Kinetic energy

$$\delta K = \frac{1}{2} \int d^3x \rho (\gamma + in\Omega)^2 |\vec{\xi}_\perp|^2$$

## Potential energy

$$\delta W = -\frac{1}{2} \int d^3x \mathbf{F} \cdot \vec{\xi}_\perp^*$$

$$\delta K_1 = -\frac{1}{2} \int d^3x \rho |\vec{\xi}_\perp|^2$$

**Growth rate equation: mode growth for  $\delta W^{\text{re}} < 0$**

$$(\gamma^{\text{re}})^2 = (\delta W_K^{\text{re}} + \delta W_F^{\text{re}} + \delta W_{vb} + \delta W_{\text{rot}}^{\text{re}}) / \delta K_1$$

$$\delta W_K = -\frac{1}{2} \int d^3x \mathbf{F}^K \cdot \vec{\xi}_\perp^* \quad \mathbf{F}^K = -\nabla \cdot \mathbf{p}^{\text{kinetic}}$$

$$\delta W_{\text{rot}} = \delta W_\Omega + \delta W_{d\Omega} + \delta W_{cf} + \delta K_2$$

$$\begin{aligned} \delta W_F^p &= -\frac{1}{2} \int d^3x \mathbf{F}^p \cdot \vec{\xi}_\perp^* \\ &= \frac{1}{2} \int d^3x \left[ (\vec{\xi}_\perp \cdot \nabla P) \nabla \cdot \vec{\xi}_\perp^* + \Gamma P |\nabla \cdot \vec{\xi}|^2 - \Gamma P (\nabla \cdot \vec{\xi}) (\nabla \cdot \vec{\xi}_\parallel^*) \right] + S_F^p \end{aligned}$$

$$\delta W_F^j = -\frac{1}{2} \int d^3x \mathbf{F}^j \cdot \vec{\xi}_\perp^* = \frac{1}{2} \int d^3x |Q|^2 + S_F^j$$

$$\delta W_F^Q = -\frac{1}{2} \int d^3x \mathbf{F}^Q \cdot \vec{\xi}_\perp^* = \frac{1}{2} \int d^3x \left[ J_\parallel \hat{\mathbf{b}} \cdot \vec{\xi}_\perp^* \times \mathbf{Q}_\perp - \frac{Q_\parallel}{B} (\vec{\xi}_\perp^* \cdot \nabla P) \right]$$

$$S_F^p = -\frac{1}{2} \int [(\vec{\xi}_\perp \cdot \nabla P) + \Gamma P \nabla \cdot \vec{\xi}] \vec{\xi}_\perp^* \cdot d\mathbf{s}$$

$$S_F^j = \frac{1}{2} \int B Q_\parallel \vec{\xi}_\perp^* \cdot d\mathbf{s}$$

## Coriolis - $\Omega$

$$\delta W_\Omega = \frac{1}{2} \int d^3x \left[ -2\rho\Omega(\gamma + in\Omega) \mathbf{Z} \times \vec{\xi}_\perp \cdot \vec{\xi}_\perp^* \right]$$

## Coriolis - $d\Omega/d\rho$

$$\delta W_{d\Omega} = \frac{1}{2} \int d^3x R \left( 2\rho\Omega (\vec{\xi}_\perp \cdot \nabla\Omega) \vec{\xi}_{\perp R}^* \right)$$

## Centrifugal

$$\delta W_{cf} = \frac{1}{2} \int d^3x R \Omega^2 \nabla \cdot (\rho \vec{\xi}_\perp) \vec{\xi}_{\perp R}^*$$

## Differential kinetic

$$\delta K_2 = -\frac{1}{2} \int d^3x \rho (\omega + n\Omega)^2 |\vec{\xi}_\perp|^2$$